

Crystal structure of kanemite, $\text{NaHSi}_2\text{O}_5 \cdot 3\text{H}_2\text{O}$, from the Aris phonolite, Namibia

LAURENCE A.J. GARVIE,^{1,*} BERTRAND DEVOUARD,^{1,†} THOMAS L. GROU,² FERNANDO CÁMARA,^{1,‡}
AND PETER R. BUSECK^{1,2}

¹Department of Geology, Arizona State University, Tempe, Arizona 85287-1404, U.S.A.

²Department of Chemistry/Biochemistry, Arizona State University, Tempe, Arizona 85287, U.S.A.

ABSTRACT

Kanemite was studied by single-crystal X-ray diffraction. The mineral, ideally $\text{NaHSi}_2\text{O}_5 \cdot 3\text{H}_2\text{O}$, is orthorhombic (space group *Pbcn*); unit-cell parameters are $a = 4.946(3)$, $b = 20.502(15)$, $c = 7.275(3)$ Å, with $Z = 4$. The structure is solved and refined to an R value of 0.058 for 825 independent reflections. The arrangement of atoms consists of alternating (010) sheets of corrugated $[\text{Si}_2\text{O}_4\text{OH}]_n^-$ and hydrated Na. The silicate sheets contain six-membered rings of $\text{HOSiO}_3\text{-SiO}_4$ units. Sodium atoms coordinate to six water molecules, forming layers of distorted octahedra. Residual electron densities were located that give reasonable positions for four H atoms. One H is part of a silanol group, and the other three H atoms are associated with water bonded to Na. Bonding between the silicate and Na sheets is through hydrogen bonding from H of the Na layer to O of the silicate sheet.

INTRODUCTION

Interest in kanemite stems from its high charge density (higher than clays), reactivity between the silicate sheets, and potential uses as a catalyst support and novel absorbent (Beneke and Lagaly 1977; Yanagisawa et al. 1990; Keene et al. 1996). In addition, kanemite is used as the starting compound for the synthesis of the mesoporous material FSM-16, which has novel catalytic and absorption properties (Yanagisawa et al. 1990; Branton et al. 1996; Inagaki et al. 1996a, 1996b; Ishikawa et al. 1996; Yamamoto et al. 1996; Yoshida et al. 1997; Sakamoto et al. 1998). An Al phosphate with the kanemite structure has been also synthesized (Cheng et al. 1997; Kimura et al. 1998). Like kanemite, the aluminophosphate layers are able to reorganize and condense to form porous materials when the interlayer ions are exchanged by surfactant cations. To understand the structural changes that take place during the exchange and intercalation reactions of kanemite and the related aluminophosphate, the details of its crystal structure must be determined.

Kanemite is a hydrated layer sodium silicate (Johan and Maglione 1972) that forms a series with the sodium silicate hydrates makatite, octosilicate, magadiite, and kenyaite. This series can be written $\text{Na}_2\text{O}(\text{SiO}_2)_x(\text{H}_2\text{O})_y$, $x = 4$ to 22 and $y = 5$ to 10 (Almond et al. 1997). Within this series, only the structure of makatite is known (Annehed et al. 1982). Kanemite

was first found in trona on the northeastern edge of Lake Chad (Johan and Maglione 1972), and it can easily be synthesized (Kalt and Wey 1968; Beneke and Lagaly 1977; Keene et al. 1996). It has been identified in peralkaline rocks of the Lovozero massif, Kola peninsula (Khomyakov 1995) and in recent sediments of Lake Bogoria, Kenya (Perinet et al. 1982).

In the absence of suitable crystals for single-crystal structural studies, the kanemite structure has been studied by ¹H, ²³Na, and ²⁹Si NMR (Apperley 1995; Almond et al. 1996, 1997; Hayashi 1997; Hanaya and Harris 1998). Despite the recent interest in kanemite, its structure is not known, although Apperley et al. (1995) thought it is similar to KHSi_2O_5 . Here we describe the structure of kanemite.

OCCURRENCE

The Aris phonolite is located about 25 km south of Windhoek, Namibia. The samples were collected from a quarry being mined for road and railway ballast. The quarrying ceased in 1996 so further collecting will be difficult. The phonolite is highly vesicular, fine-grained, aphyric and consists of alkali feldspars, nepheline, and acmite with minute accessory apatite, zircon, and monazite (von Knorring and Franke 1987). Detailed geochemistry of the nearby phonolites from the Klinghardt Mountains is given by Marsh (1987). The vesicles in our samples range from <1 mm to over 10 cm in diameter. Many are filled with fluid and appear to “burst” when the rocks are split. In addition to kanemite, the vesicles contain villiaumite, natrolite, aegerite, microcline, apophyllite, analcime, fluorite, hydroxyapatite, galena, sphalerite, makatite, quartz, about a dozen less well-characterized or new species, and the second occurrence of taperssuatsiaite (von Knorring et al. 1992; Cámara et al., in preparation).

Kanemite from Aris is rare; only 25 crystals were found in ca. 200 kg of rock. In contrast, another sodium silicate makatite

*E-mail: lgarvie@asu.edu

†Present address: Département de Géologie, CNRS-UMR 6524, Magmas et Volcans, 5 rue Kessler, F-63038 Clermont-Ferrand cedex, France.

‡Present address: Laboratoire de Structure et Propriétés de l'Etat solide, Bat C6, Université des Sciences et Technologies de Lille, F-59655, Villeneuve d'Ascq Cedex, France.



FIGURE 1. Photograph of the largest kanemite crystal (white) found to date (D. Shannon collection). The radiating crystals groups are tapersuutsiaite. Kanemite crystal is 3 × 10 mm.

(Na₂Si₄O₉·5H₂O) is comparatively common, forming well-crystallized masses up to 10 cm in diameter. Although makatite can be transformed into kanemite (Beneke and Lagaly 1977), the two were never found in the same vug. The kanemite ranges from less than 1 mm to 1 cm long (Fig. 1) and resembles gypsum in its luster, hardness, and color. Fresh crystals from wet vugs are clear but rapidly turn white and opaque when dry. The crystals grow from the surfaces of the vugs without accessory phases growing on them. Microprobe data of the kanemite shows only Na, Si, O, and minor Ca, and the powder X-ray diffraction data are similar to that from Lake Chad (powder diffraction file—PDF 25-1309).

The crystals are euhedral and grew in two morphologies: tabular flattened parallel to (010) and elongated along [100]. Only faces of the pinacoid {010} and rhombic prisms {110} and {011} are visible. Kanemite from Aris has good cleavage parallel to (010), and the crystals are striated parallel to [100]. Similar morphologies are visible for the Lake Bogoria and Lake Chad kanemites (Johan and Maglione 1972; Perinet et al. 1982). The dried crystals have a pearly to silky luster and appear to be stable, unlike the Russian material (Khomyakov 1995, p. 92).

CRYSTAL-STRUCTURE REFINEMENT

Attempts were made to obtain single-crystal data from the air-dried kanemite but were without success, although the powder X-ray diffraction pattern is consistent with well-crystallized material (PDF 25-1309). It is possible that upon drying the crystals deformed slightly so they no longer were single crystals. A crystal was located in a wet vug and was immediately cut into small plates and sealed while wet into a glass capillary. The crystal cleaved into thin plates during preparation, and X-ray data were acquired from a flake with dimensions 0.375 mm × 0.100 mm × 0.075 mm using a Siemens P3 autodiffractometer. Methods of data collection and the results of the structure refinement are given in Table 1. The cell set-

tings and space group differ from those determined for the Lake Chad kanemite (Johan and Maglione 1972).

Table 2 contains the positional and equivalent isotropic displacement parameters. Selected bond distances and angles are given in Tables 3 and 4. Anisotropic displacement parameters are given in Table 5, and positional and equivalent isotropic displacement parameters for H atoms are in Table 6.

DESCRIPTION OF THE STRUCTURE AND DISCUSSION

Kanemite consists of silicate sheets alternating with hydrated Na sheets (Fig. 2). Using the terminology of Liebau (1987), the silicate sheet (Fig. 3) can be described as built up of unbranched *vierer* single chains (Si₄O₁₂)_n. The silicate sheets contain six-membered rings of HOSiO₃-SiO₄ units (Q³). Such polymerization is consistent with ²⁹Si NMR data, which indicate that only signals arising from Q³ environments occur and only one Si site is present (Hayashi 1997). The chains condense to form sheets perpendicular to the *z*-axis. Viewed along [100], the sheets have a puckered appearance (Figs. 2 and 3). The O2 atoms point into the interlayer regions whereas O1 and O3 are bridging O atoms and connect the SiO₄ tetrahedra.

The Na sheet is composed of hydrated Na in a distorted octahedral coordination (Table 3). These octahedra share edges through O4, forming (Na₂O₆)ⁿ⁻ units parallel to the *z*-axis (Fig. 4). These chains connect via corner sharing through O5 to form the hydrated Na sheet. The single Na site is consistent with NMR data (Almond et al. 1996; Hayashi 1997) although not with the NMR results of Keene et al. (1996), which show that there are two Na

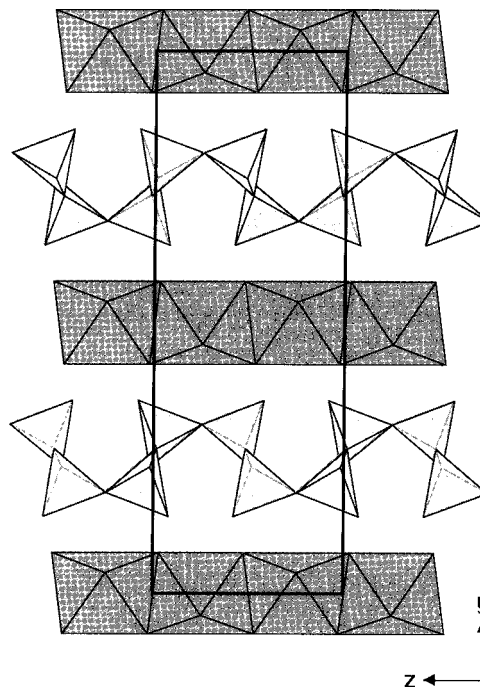


FIGURE 2. Crystal structure of kanemite projected down [100]. The dark layer represents the NaO₆ octahedra and the light layer the SiO₄ tetrahedra. The rectangle depicts the unit cell.

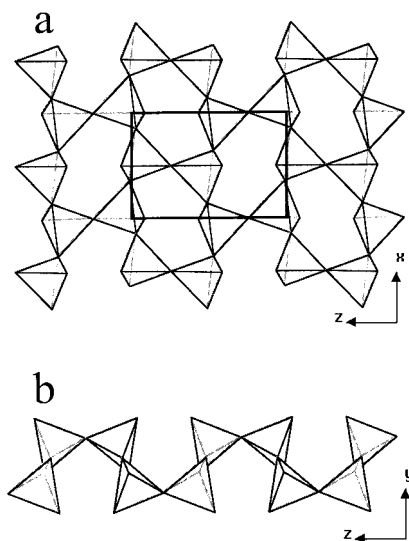


FIGURE 3. Two views of the silicate sheet: (a) projected down [010], showing the six-membered SiO₄ rings, and (b) down [100], showing the puckering of the sheet. The rectangle in a indicates the unit cell.

TABLE 1. Crystal data and results of structure refinement of kanemite

Crystal size	0.375 × 0.100 × 0.075 mm
Crystal system	Orthorhombic
Space group	<i>Pbcn</i>
Unit-cell dimensions (Å)	<i>a</i> = 4.946(3), <i>b</i> = 20.502(15), <i>c</i> = 7.275(3)
Volume	737.7(8) Å ³
Z	4
Range for data collection	1.99 to 35.08°
Monochromator	Graphite
Wavelength	0.71073 Å
Temperature	293(2) K
Measurement method	Scan
Measurement speed	1.50 to 14.65°/min. in ω
Measurement range	1.60 in ω
Reflections collected	6211 / (1628 unique) with R_{int} = 0.1504
Index ranges	0 ≤ <i>h</i> ≤ 7, -33 ≤ <i>k</i> ≤ 33, -11 ≤ <i>l</i> ≤ 11
Absorption correction	None
Structure solution	Direct methods (XS in SHELXTL PC 5.03)
Refinement method	Full-matrix least-squares on F^2
Data	1628
Restraints	5
Parameters	81
$R\{I > 2\sigma(I)\}$	0.0582
<i>R</i> _w	0.1185
Goodness-of-fit on F^2	0.996
Largest peak on difference map	0.524 e/Å ³ (+), 0.396 e/Å ³ (-)

TABLE 2. Atomic coordinates (× 10⁴) and equivalent isotropic displacement parameters (Å² × 10³) of kanemite

Atom	<i>x</i>	<i>y</i>	<i>z</i>	<i>U</i> _{eq}
Si1A	497(2)	2925(1)	391(1)	13(1)
Si1B	497(2)	2925(1)	391(1)	13(1)
Na1	5000	5115(1)	-2500	29(1)
O1A	0	3128(2)	2500	30(1)
O1B	0	3128(2)	2500	30(1)
O2A	42(4)	3571(1)	-790(2)	23(1)
O2B	42(4)	3571(1)	-790(2)	23(1)
O3A	-1438(4)	2326(1)	-181(3)	26(1)
O3B	-1438(4)	2326(1)	-181(3)	26(1)
O4A	4876(6)	5754(1)	267(4)	33(1)
O4B	4876(6)	5754(1)	267(4)	33(1)
O5	0	5411(3)	-2500	67(3)

Note: *U*_{eq} is defined as one third of the trace of the orthogonalized *U*_i tensor.

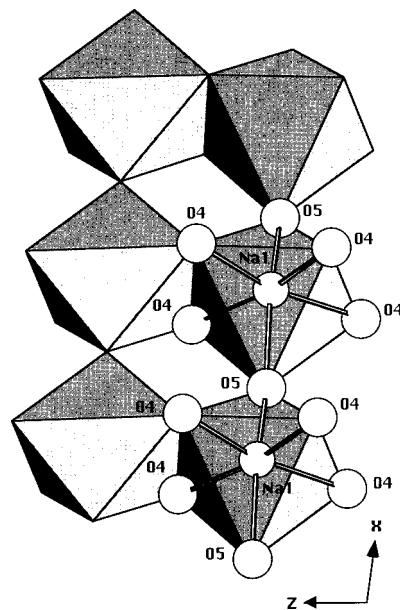


FIGURE 4. Structural environment of Na showing the edge sharing octahedra along *z* and corner sharing along *x*.

sites, one closely associated with protons and the other is neither attached to or close to a source of protons. Under the conditions of the X-ray refinement, only one Na site was detected. It is possible that for slightly dehydrated samples, or samples equilibrated in air, some of the Na atoms are preferentially dehydrated and thus produce the range of Na sites observed by ²³Na NMR. Such a conclusion was reached by Hanaya and Harris (1998) who resolved signals from three different Na sites, but only because of different hydration states. The refined electron density at the Na site is less than 11 e⁻ (10.67 e⁻). The refined value agrees with a site population represented by Na_{0.8}, Ca_{0.1}, and □_{0.1} (where □ stands for vacancy). Some Ca is found in kanemite reaching up to 0.1 apfu in agreement with the refined site scattering.

Residual electron densities were located that give reasonable positions for most of the hydrogen atoms. Four separate H atoms were located (Table 6): H2A is associated with O2, which is bonded to Si forming a hydroxy group; and H4A, H4B, and H5A are bonded to O4, O5, and Na, respectively (Fig. 5). These two types of H atoms are consistent with ¹H NMR data (Hayashi 1997). The H atoms in kanemite were added to the model and their coordinates refined with a fixed full occupancy for all but H2A, which shows a fairly low electron density. In fact, H2A shows an electron density less than the Si-O2 and Si-O3 lone pair electrons, which were the highest peaks in the Fourier difference map after the three hydrogen maxima.

Hydrogen atoms H4A and H4B appear to be in reasonable positions bonded to O4 at distances of 0.821 and 0.832 Å, respectively. The H4A-O-H4B angle is 115.06°. Each H4 is pointing to O2, which acts as acceptor and is at a distance of 2.824 and 2.893 Å from the O4 donors, and at 2.012 and 2.062 Å from the H atoms: they represent moderate hydrogen bonds (Jeffrey 1997). H-O distances are shorter than the expected values. Because H4A and H4B have high atomic-displacement

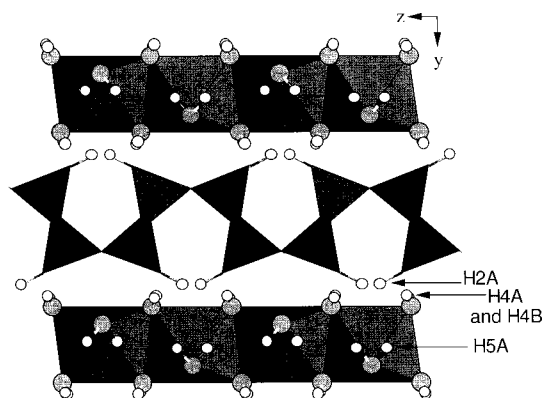


FIGURE 5. Projection of the kanemite structure down [100] showing the locations of the H atoms. H atoms are shown by small white circles and O atoms by larger gray circles.

parameters (adp) their actual bond distance must be slightly underestimated.

H5A is bonded to O5 at a distance of 0.931 Å with an H5A-O5-H5A angle of 83.04°. This small angle is probably due to local charge requirements. The two H atoms point toward the alternating cavities in the Na layer (Fig. 5), avoiding extra charge from the silicate layer that is already linked through the H4A and H4B hydrogen bonds. The positions of those maxima are at the correct distance to represent an O-H bond. However, the H5A-O5-H5A angle is rather low and the two H atoms are at a distance of 1.23 Å, which is too short because of H-H charge repulsion. The O5 has a high adp and has a refined site scattering less than 8 e⁻. This high adp points to a disorder that is probably due to a heterogeneous distribution of water vacancies within the Na layer. Therefore, it is difficult to accurately locate the hydrogen maxima.

The H atom H2A bonded to O2 must be half occupied because the residual electron density is lower than the maximum corresponding to the Si-O bonding. In addition, full H2 occupancy would force the two H atoms to within 0.77 Å of each other. Full H2A occupancy gives the ratio Na:2Si:8H:8O or

TABLE 3. Selected interatomic distances [Å] in kanemite

Si-O2	1.595(2)	Na-O4	2.403(3)
Si-O3*	1.608(2)	Na-O4†	2.413(3)
Si-O1	1.6086(13)	Na-O5	2.546(2)
Si-O3	1.611(2)	<Na-O>	2.454
	1.6056	Vol (Å ³)	18.55
Vol (Å ³)	2.118	OAV‡	129.156
TAV	8.564	OQE‡	1.0417
TQE‡	1.0021	Na-Na§	3.6682(16)
		Na-H5A	2.52(4)
O2-H2A	1.0(2)		
O5-H5A	0.93(5)		

Note: TAV = tetrahedral angle variance; TQE = tetrahedral quadratic elongation; OAV = octahedral angle variance; OQV = octahedral quadratic elongation.

*Symmetry transformations used to generate equivalent atoms: x+1/2, -y+1/2, -z.

† x, -y+1, z-1/2.

‡ following Robinson et al. (1971).

§ x+1, -y+1, -z-1.

NaH₂Si₂O₅·3H₂O, as opposed to the accepted NaHSi₂O₅·3H₂O; a nonprotonated tetrahedral layer would be (Si₂O₅)²⁻ and a fully protonated one Si₂O₅(OH)₂, which would be neutral.

Bond-valence calculations obtained with the Eutax v1.5 program using the parameters calculated by Bresse and O'Keeffe (1991) are presented in Table 7. When the H atoms are excluded from the calculation, O2 is underbonded, missing 0.92 v.u. from the ideal value of 2.0 v.u. Considering that O2 is bonded as a donor to H2A at a distance of 0.99 Å (with half occupancy) and as an acceptor of H4A and H4B at 2.012 and 2.062 Å, the bond strength yield by the hydrogen bonding (0.7 v.u.) nearly fulfills the charge requirement of this oxygen. Longer O4-H4A and O4-H4B distances would yield higher valence strengths to this O atom. Bond valence calculations without considering the H atoms also show that O4 and O5 are strongly underbonded, with bond strengths of 0.383 and 0.265 v.u. as would be expected for water molecules. This is complemented by the bond strength yield by two H atoms.

The high water content of kanemite, and the ease with which the Na can be cation exchanged, is consistent with a hydrated Na sheet. Hayashi (1997) considers three types of water in

TABLE 4. Selected interatomic angles (°) in kanemite

O2-Si-O3*	110.33(12)	Na -Na-Na§	165.17(12)	O4§-Na-Na#	124.90(11)
O2-Si-O1	106.10(14)	O4†-Na-O4	113.90(14)	O5 -Na-Na#	91.76(2)
O3*-Si-O1	108.54(9)	O4†-Na-O4‡	80.78(10)	O4†-Na-H5A	80.8(8)
O2-Si-O3	114.17(12)	O4-Na-O4‡	165.10(10)	O4-Na-H5A	101.5(11)
O3*-Si-O3	106.96(7)	O4‡-Na-O4§	84.70(14)	O4†-Na-H5A	80.8(8)
O1-Si-O3	110.65(12)	O4-Na-O5	83.97(10)	O4‡-Na-H5A	77.5(11)
Si-O1-Si**	150.0(2)	O4‡-Na-O5	101.58(12)	O4§-Na-H5A	99.4(8)
Si††-O3-Si	145.96(14)	O4§-Na-O5	98.70(12)	O5 -Na-H5A	161.7(8)
Si-O2-H2A	148(10)	O4†-Na-O5	83.97(10)	O5-Na-H5A	21.2(10)
		O4-Na-O5	81.10(10)	Na#-Na-H5A	75.7(9)
		O4‡-Na-O5	98.70(12)	Na§-Na-H5A	103.8(9)
		O5 -Na-O5	152.4(3)	Na-O4-Na§	99.22(10)
		O4†-Na-Na#	40.50(7)	Na‡‡-O5-Na	152.4(3)
		O4-Na-Na#	154.31(11)	Na‡‡-O5-H5A	82(2)
		O4†-Na-Na#	40.28(7)	Na-O5-H5A	78(2)

Symmetry transformations used to generate equivalent atoms:

* x+1/2, -y+1/2, -z.

|| x+1, y, z.

† -x+1, y, z-1/2.

** -x, y, z+1/2.

‡ x, -y+1, z-1/2.

†† x-1/2, -y+1/2, -z.

§ -x+1, -y+1, -z.

‡‡ x-1, y, z.

-x+1, -y+1, -z-1.

TABLE 5. Anisotropic displacement parameters ($\text{\AA}^2 \times 10^3$) of kanemite

	U_{11}	U_{22}	U_{33}	U_{23}	U_{13}	U_{12}
Si1A	10(1)	18(1)	11(1)	0(1)	1(1)	2(1)
Si1B	10(1)	18(1)	11(1)	0(1)	1(1)	2(1)
Na1	34(1)	29(1)	25(1)	0	0(1)	0
O1A	33(2)	42(2)	14(1)	0	4(1)	0
O1B	33(2)	42(2)	14(1)	0	4(1)	0
O2A	31(1)	23(1)	14(1)	3(1)	0(1)	3(1)
O2B	31(1)	23(1)	14(1)	3(1)	0(1)	3(1)
O3A	11(1)	25(1)	43(1)	-8(1)	-1(1)	-1(1)
O3B	11(1)	25(1)	43(1)	-8(1)	-1(1)	-1(1)
O4A	37(2)	23(1)	39(1)	-2(1)	1(1)	-1(1)
O4B	37(2)	23(1)	39(1)	-2(1)	1(1)	-1(1)
O5	29(3)	60(4)	111(6)	0	3(3)	0

The anisotropic displacement factor exponent takes the form: $-2\pi^2 (h^2 a^2 U_{11} + \dots + 2 h k a^* b^* U_{12})$.

TABLE 6. Hydrogen coordinates ($\times 10^4$) and isotropic displacement parameters ($\text{\AA}^2 \times 10^3$) of kanemite

	x	y	z	U_{eq}
H2A	193(5)	3795(6)	-1989(3)	36(12)
H4A	6450(10)	4020(2)	-510(6)	65(16)
H4B	3640(11)	4060(2)	-430(7)	85(19)
H5A	67(8)	5071(2)	-3347(5)	170(7)

TABLE 7. Bond-valence calculations results from UTAX for kanemite

	Si	Na	Σ
O1	1.037 $\times 2$		2.074
O2	1.077		1.077
O3	1.041		
	1.030		2.071
O4		0.194 $\times 2$	0.388
		0.189 $\times 2$	0.383
O5		0.132 $\times 2$	0.264
Σ	4.185	1.030	

kanemite: external surface water, interlayer water, and hole water within the puckered regions of the silicate sheet. The relationship between the interlayer water and Na⁺ can be considered relative to the water's mobility (Hayashi 1997): mobile water, mobile water that spends part of the time coordinated to Na⁺, and water rigidly coordinated to Na⁺. Almond et al. (1997) considers the interlayer water to be mobile. Some interlayer water can easily be removed by gentle heating (Johan and Maglione 1972; Perinet et al. 1982; Apperley et al. 1995; Hayashi 1997), which results in a decrease in the spacing between the silicate and Na sheets. This decrease is evident from the (020) reflection, measured by powder X-ray diffraction, which decreases from 10.27 Å for the air-dried and wet kanemite to 8.615 Å after heating at 60° for 5 min. For the hydrostatic conditions at which the X-ray data were acquired, the water molecules are fixed, allowing the positions of their O atoms to be determined. In addition, the Na-O bond distances in kanemite are consistent with octahedrally coordinated Na (Table 3).

The silicate and Na sheets are probably connected via hydrogen bonds. Bonding of the two sheets was thought to be through O atoms of adjacent SiO₄ sheets of the type Si-O-H ... O-Si (Almond et al. 1997; Hayashi 1997) as found in KHSi₂O₅ (Le Bihan et al. 1971). Such a model is probably not feasible

because of the large distance, 5.97 Å, between the closest O atoms of adjacent Si layers. A more plausible model for the cohesion between the sheets is that of hydrogen bonding between the H of the H₂O coordinated to Na⁺ and the O of the silicate sheets. One possibility is Si-O2 ... H4-O4-Na, with O2 ... H4 and O2 ... H4 bond lengths of ca. 2 and 0.8 Å, respectively. A similar bonding scheme is found in Ni-vermiculite in which the Ni is octahedrally coordinated to H₂O, and the water is oriented to form a strong H bond to the adjacent clay surface (Skipper et al. 1991).

Kanemite shows structural and physical similarities to the clay minerals: reversible hydration and dehydration, and exchange by inorganic and organic cations. Water is associated with the Na sheet but can also occur within the channels of the silicate sheet. The NMR data of Hayashi (1997) shows that mild drying affects the mobility, amount, and location, of water molecules, the mobility of the Na⁺, and the structure of the silicate sheet. We refined the structure of a wet sample, but the structure may differ for dried samples through loss of the water from the channels of the corrugated silicate sheets. In contrast to published NMR results, we find that Na⁺ is coordinated directly to water molecules and that the silicate and Na sheets are bonded through hydrogen bonds of the form Si-O2 ... H4-O4-Na.

ACKNOWLEDGMENTS

We thank D. Shannon (Tempe, Arizona) for the samples of kanemite and M. O'Keeffe (ASU) for help with the UTAX program. This work was supported by National Science Foundation grant no. EAR-9706359.

REFERENCES CITED

- Almond, G.G., Harris, R.K., Franklin, K.R., and Graham, P. (1996) A ²³NMR study of hydrous layered silicates. *Journal of Materials Chemistry*, 6, 843–848.
- Almond, G.G., Harris, R.K., and Franklin, K.R. (1997) A structural consideration of kanemite, octosilicate, magadiite and kenyaite. *Journal of Materials Chemistry*, 7, 681–687.
- Annehed, H., Fäth, L., and Lincoln, F.J. (1982) Crystal structure of synthetic makatite Na₂Si₂O₇(OH)₂·4H₂O. *Zeitschrift für Kristallographie*, 159, 204–210.
- Apperley, D.C., Hudson, M.J., Keene, M.T.J., and Knowles, J.A. (1995) Kanemite (NaHSi₂O₅·3H₂O) and its hydrogen-exchanged form. *Journal of Materials Chemistry*, 5, 577–582.
- Beneke, K. and Lagaly, G. (1977) Kanemite—innercrystalline reactivity and relations to other sodium silicates. *American Mineralogist*, 62, 763–771.
- Branton, P.J., Kaneko, K., Setoyama, N., Sing, K.S.W., Inagaki, S., and Fukushima, Y. (1996) Physisorption of nitrogen by mesoporous modified kanemite. *Langmuir*, 12, 599–600.
- Brese, N.E. and O'Keeffe, M. (1991). Bond-valence parameters for solids. *Acta Crystallographica*, B47, 192–197.
- Cheng, S., Tzeng, J.N., and Hsu, B.Y. (1997) Synthesis and characterization of a novel layered aluminophosphate of kanemite-like structure. *Chemistry of Materials*, 9, 1788–1796.
- Hanaya, M. and Harris, R.K. (1998) Two dimensional ²³Na MQ MAS NMR study of layered silicates. *Journal of Materials Chemistry*, 8, 1073–1079.
- Hayashi, S. (1997) Solid-state NMR study of locations and dynamics of interlayer cations and water in kanemite. *Journal of Materials Chemistry*, 7, 1043–1048.
- Inagaki, S., Koiwai, A., Suzuki, N., Fukushima, Y., and Kuroda, K. (1996a) Syntheses of highly ordered mesoporous materials, FSM-16, derived from kanemite. *Bulletin of the Chemical Society of Japan*, 69, 1449–1457.
- Inagaki, S., Sakamoto, Y., Fukushima, Y., and Terasaki, O. (1996b) Pore wall of a mesoporous molecular sieve derived from kanemite. *Chemistry of Materials*, 8, 2089–2095.
- Ishikawa, T., Matsuda, M., Yasukawa, A., Kandori, K., Inagaki, S., Fukushima, T., and Kondo, K. (1996) Surface silanol groups of mesoporous silica FSM-16. *Faraday Transactions*, 92, 1985–1989.
- Jeffrey, G.A. (1997) *An introduction to hydrogen bonding*. Oxford University Press, 303 p.
- Johan, Z. and Maglione, G.F. (1972) La Kanemite, nouveau silicate de sodium hydraté de néoformation. *Bulletin de la Société Française de Minéralogie et de Cristallographie*, 95, 371–382.
- Kalt, A. and Wey, R. (1968) Composés interfoliaires d'une silice hydratée cristallisée.

- Bulletin de Groupe Française des Argiles, 20, 205–214.
- Keene, M.T.J., Knowles, J.A., and Hudson, M.J. (1996) The reversible extraction of the hexaminecobalt (III) cation by kanemite (NaHSi₂O₅·3H₂O): enhanced extraction in the presence of a cationic surfactant. *Journal of Materials Chemistry*, 6, 1567–1573.
- Kimura, T., Sugahara, Y., and Kuroda, K. (1998) Synthesis of mesoporous aluminophosphates and their adsorption properties. *Microporous and Mesoporous Materials*, 22, 115–126.
- Khomyakov, A.P. (1995) *Mineralogy of Hyperagpaitic Alkaline Rocks*, 223 p. Oxford University Press, Oxford.
- Le Bihan, M.T., Kalt, A., and Wey, R. (1971) Étude structurale de KHSi₂O₅ et H₂Si₂O₅. *Bulletin de la Société Française de Minéralogie et de Cristallographie*, 94, 15–23.
- Liebau, F. (1985) *Structural chemistry of the silicates. Structure, bonding, and classification*, 347 p. Springer-Verlag, Berlin.
- Marsh, J.S. (1987) Evolution of a strongly differentiated suite of phonolites from the Klinghardt Mountains, Namibia. *Lithos*, 20, 41–58.
- Perinet, G., Tiercelin, J.J., and Barton, C.E. (1982) Présence de kanemite dans les sédiments récents du lac Bogoria, Rift Gregory, Kenya. *Bulletin de Minéralogie*, 105, 633–639.
- Robinson, K., Gibbs, G.V., and Ribbe, P.H. (1971) Quadratic elongation: a quantitative measure of distortion in coordination polyhedra. *Science*, 172, 567–570.
- Sakamoto, Y., Inagaki, S., Ohsuna, T., Ohnishi, N., Fukushima Y., Nozue, Y., and Terasaki, O. (1998) Structure analysis of mesoporous materials “FSM-16”—Studies by electron microscopy and x-ray diffraction. *Microporous and Mesoporous Materials*, 21, 589–596.
- Skipper, N.T., Soper, A.K., and McConnell, J.D.C. (1991) The structure of interlayer water in vermiculite. *Journal of Chemical Physics*, 94, 5751–5760.
- von Knorring, O. and Franke, W. (1987) A preliminary note on the mineralogy and geochemistry of the Aris phonolite, SWA/Namibia. *Communications of the Geological Survey of S.W. Africa/Namibia*, 3, 61.
- von Knorring, O., Petersen, O.V., Karup-Møller, S., Leonardsen, E.S., and Condliffe, E. (1992) Taperssuatsiaite from Aris phonolite, Windhoek, Namibia. *Neues Jahrbuch für Mineralogie Monatshefte*, 145–152.
- Yamamoto, T., Shido, T., Inagaki, S., Fukushima, Y., and Ichikawa, M. (1996) Ship-in-bottle synthesis of [Pt₁₅(CO)₃₀]²⁻ encapsulated in ordered hexagonal mesoporous channels of FSM-16 and their effective catalysis in water-gas shift reaction. *Journal of the American Chemical Society*, 118, 5810–5811.
- Yanagisawa, T., Shimizu, T., Kuroda, K., and Kato, C. (1990) The preparation of alkyltrimethylammonium-kanemite complexes and their conversion to microporous materials. *Bulletin of the Chemical Society of Japan*, 63, 988–992.
- Yoshida, H., Kimura, K., Inaki, Y., and Hattori, T. (1997) Catalytic activity of FSM-16 for photometathesis of propene. *Chemical Communications*, 129–130.

MANUSCRIPT RECEIVED DECEMBER 12, 1997

MANUSCRIPT ACCEPTED FEBRUARY 4, 1999

PAPER HANDLED BY RONALD C. PETERSON